Mathematical Sciences Letters
An International Journal

http://dx.doi.org/10.12785/msl/020305

Scattered Data Interpolation based on Dual Reciprocity Boundary Element Method with Unknown Boundary Conditions

Mahdi Sovizi[1,*] *and Isa Esfandiarpour* [2]

[1] Physics Dept., Faculty of Science, Vali-e-Asr University of Rafsanjan, P.O. Box 518, Rafsanjan, Iran
[2] Soil Science Dept., College of Agriculture, Vali-e-Asr University of Rafsanjan, P.O. Box 518, Rafsanjan, Iran

Received: 27 Feb. 2013, Revised: 2 May. 2013, Accepted: 4 May. 2013
Published online: 1 Sep. 2013

Abstract: A numerical method based on Dual Reciprocity Boundary Element Method (DRBEM) has presented to interpolate two-dimensional data with arbitrary pattern. This method is performed without specific boundary conditions. It claimed that interpolation function is true on the Poisson equation with unknown source function. The source function is estimated by radial basis functions expansion. Finally, numerical sampling has conducted on some specific functions as primary functions and interpolation values of numerical sampling have compared to primary function values in order to evaluate accuracy and precision of the method.

Keywords: Interpolation, Scattered Data, Radial Basis Functions, Dual Reciprocity Boundary Element Method.

1 Introduction

Numerical methods today's are used in many branches of science, engineering and technology as a high efficient method to simulate and solve practical problems. One of these methods is the interpolation method. Various methods have introduced for the interpolation of one-dimensional, two-dimensional and three-dimensional data with regular or non-regular configurations [1]. A numerical method is presented to interpolate two-dimensional data with arbitrary pattern. It assumed that interpolation function is valid in the Poisson equation with unknown source function. Source function has extended by radial basis functions (RBFs) [2,3,4,5,6] that will be unknown expansion coefficients. Then by using location of sampled points, a closed boundary created. After that, Green's theorem is used to change the Poisson equation into integral equation and domain integral at integral equation changes to boundary equation by expansion of source function. Finally, the unknown coefficients of the expanded source function and unknown coefficients of boundary integral equation are calculated by conventional boundary element method. The results of interpolation with primary function values compared together and comparisons results are reported to evaluate the accuracy of the proposed method. Although an interpolation technique from scattered data with specific boundary conditions was presented by reference [7], the current method is performed without specific boundary conditions where is very applicable in practical problems.

2 Numerical method

It assumed that sampling has done at N points with $X_k = (x_k, y_k)$ coordinates, $k \in \{1,...,N\}$, from $\bar{U}(X)$ quantity as a primary function. The sampled data is shown with $U_k = \bar{U}(X_k)$. Interpolation function of $U(X)$ that is an approximation from the primary function, $\bar{U}(X)$, is considered that satisfy the following differential equation:

$$\nabla^2 U(X) = Q(X) \tag{1}$$

It must be notify that in equation (1) as well as the $U(X)$, $Q(X)$ function is also unknown. In this equation $Q(X)$ plays the source role. $U(X)$ function will be able to calculate if $Q(X)$ function and appropriate boundary condition on the boundary of sampling area are known [8]. In the following, the source function will approximate by RBFs. Hence, the equation (1) converts to

* Corresponding author e-mail: msovizi@gmail.com

the appropriate integral equation and solve this integral equation by boundary element method. At first, with regard to the location of sampling points $\{X_k\}$, by connecting the outer points together, the boundary of area is formed. The closed boundary (connection of points to each other) shows with Γ and the surrounded area by the boundary is shown with Ω. The figure of Γ boundary and Ω domain is not particular and different type of figures can shape the domain but it must be notify that finally interpolation function is only estimated in the domain of the formed boundary. Two types of the formed boundaries and domains by a similar set of sampling points are shown in Fig. 1. The differential equation (1) converts into the integral equation after formation of Γ boundary and Ω domain. The second form of Green's theorem is used for this conversion as follows:

$$\int_{\Omega} \psi(X)\nabla^2\phi(X) - \phi(X)\nabla^2\psi(X)\,d\Omega = \oint_{\Gamma} \psi(X)\frac{\partial\phi(X)}{\partial n} - \phi(X)\frac{\partial\psi(X)}{\partial n}d\Gamma \tag{2}$$

The two functions of $\psi(X)$ and $\phi(X)$ are arbitrary scalar functions and $\partial/\partial n$ shows normal derivative of considered quantities that is defined as follows:

$$\partial(.)/\partial n = \hat{n}.\vec{\nabla}(.) \tag{3}$$

where $\hat{n}$ is normal vector perpendicular to the Γ boundary and is considered outward to Ω domain. Green equation corresponding to equation (1) is expressed as follows:

$$\nabla^2 G(X,X') = -\delta(X-X') \tag{4}$$

where $G(X,X')$ is Green function and $\delta(X-X')$ is the Dirac delta function. In this method, there is no restriction to choose Green function. Therefore, with regard to the problem that is a two or three dimensional problem, the simplest Green function will be selected. In two-dimensional problems, Green function is considered as $G(X,X') = -\ln|X-X'|/2\pi$. Equation (2) is rewritten for the functions $\psi(X) = G(X,X')$ and $\phi(X) = U(X)$ as follows:

$$\int_{\Omega} G(X,X')\nabla^2 U(X) - U(X)\nabla^2 G(X,X')\,d\Omega = \oint_{\Gamma} G(X,X')\frac{\partial U(X)}{\partial n} - U(X)\frac{\partial G(X,X')}{\partial n}d\Gamma \tag{5}$$

By substitution equations (1) and (4) in equation (5) it drives:

$$\int_{\Omega} G(X,X')Q(X) + U(X)\delta(X-X')\,d\Omega = \oint_{\Gamma} G(X,X')\frac{\partial U(X)}{\partial n} - U(X)\frac{\partial G(X,X')}{\partial n}d\Gamma \tag{6}$$

The second term of the left hand side of equation (6) is calculated as follows:

$$\int_{\Omega} U(X)\,\delta(X-X')\,d\Omega = C(X')\,U(X') \tag{7}$$

The coefficient $C(X')$ for the inner and outer regions of the Γ boundary is equal to:

$$C(X') = \begin{cases} 1 & X' \in \Omega \text{ and } X' \notin \Gamma \\ 0 & X' \notin \Omega \text{ and } X' \notin \Gamma \end{cases} \tag{8}$$

If X' locates on the Γ boundary, $C(X')$ can be obtained from the following equation:

$$C(X') = -\oint_{\Gamma} \frac{\partial G(X,X')}{\partial n}d\Gamma,\ X' \in \Gamma \tag{9}$$

Since in the equation (9) $X' \in \Gamma$, so the integral in the point $X = X'$ will be singular, therefore, it's Cauchy Principal Value (CPV) needs to be calculated. Introducing Eq. (7) in Eq. (6) gives:

$$C(X')U(X') = -\int_{\Omega} G(X,X')Q(X)\,d\Omega + \oint_{\Gamma} G(X,X')\frac{\partial U(X)}{\partial n} - U(X)\frac{\partial G(X,X')}{\partial n}d\Gamma \tag{10}$$

Each integrals of equation (10) can be shown as follows:

$$I_{\Omega}(X') = \int_{\Omega} G(X,X')Q(X)\,d\Omega \tag{11}$$

$$I_{1\Gamma}(X') = \oint_{\Gamma} G(X,X')\frac{\partial U(X)}{\partial n}d\Gamma \tag{12}$$

$$I_{2\Gamma}(X') = \oint_{\Gamma} U(X)\frac{\partial G(X,X')}{\partial n}d\Gamma \tag{13}$$

By considering the integral equation (10), if $Q(X)$ is known in the Ω domain, also $U(X)$ and $\partial U(X)/\partial n$ are known on the Γ boundary, value of $U(X')$ will be able to calculate at any arbitrary point in the Ω domain. As a result, $Q(X)$ at the domain of Ω, also $U(X)$ and $\partial U(X)/\partial n$ on the Γ boundary must be estimate. In the following, a numerical method to calculate these functions based on DRBEM will provide.

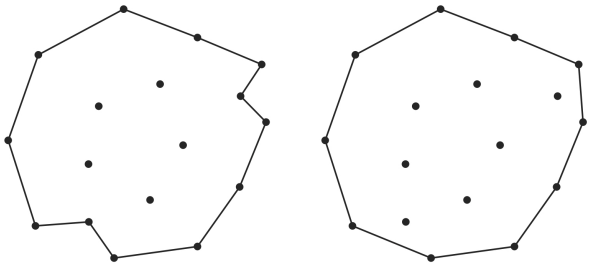

Fig. 1. The formation of two different boundaries with a uniform set of sample points.

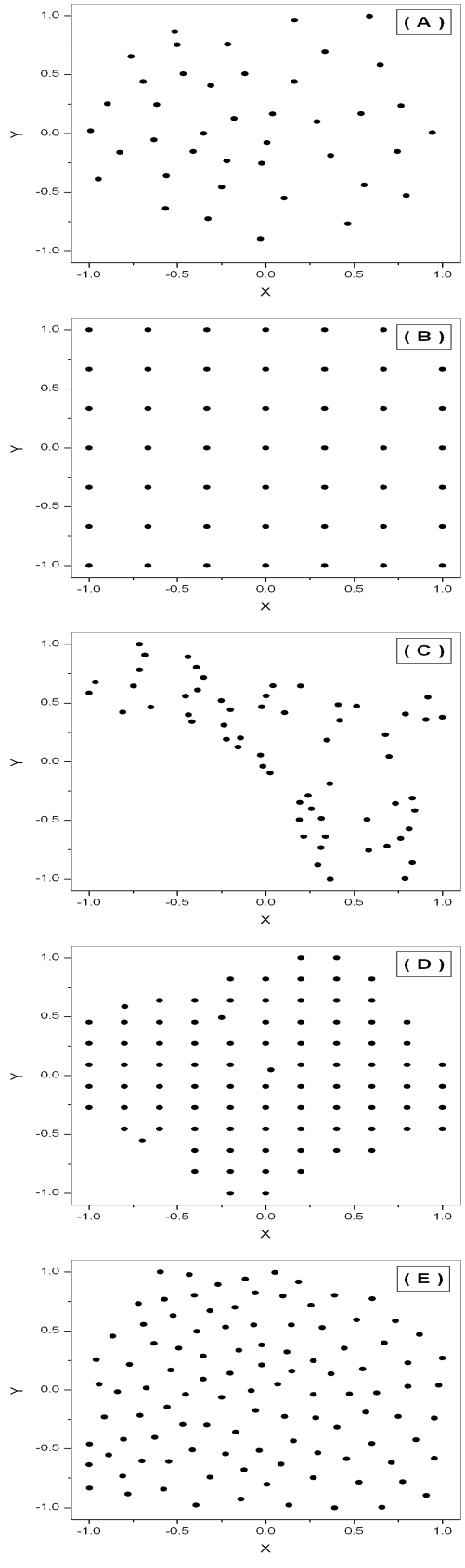

Fig. 2. Different point's arrangement (A: 41, B: 49, C: 60, D: 91, E: 106 points.)

3 Domain integral

The expressed integral in the equation (11) must be performed on total considered domain. There will be two problems in numerical calculation of this integral if assume that $Q(X)$ is known. First, Ω domain typically has irregular shape. Secondly, if the observing point X' is selected in the Ω domain, the integral will be singular. In order to solve these two problems, the integral will be converted to boundary integral by expansion of $Q(X)$ function based on radial basis functions. This expansion is expressed as follows [9,10]:

$$Q(X)=\sum_{k=1}^{N}\alpha_k Q_k^{(m)}(X,X_k) \tag{14}$$

where $Q_k^{(m)}(X,X_k)$ is a m order polynomial of R_k as follows:

$$Q_k^{(m)}(X,X_k)=Q_k^{(m)}(R_k)=\sum_{l=0}^{m}R_k^l,\quad R_k=|X-X_k| \tag{15}$$

In this equation, X_k shows the location of the sampling points and summation of the equation (14) is carried out on all these points. Coefficients of α_k in equation (14) are unknown. In addition, it can be seen that the functions of $Q_k^{(m)}(R_k)$ play role of source in the following differential equation:

$$\nabla^2 U_k^{(m)}(R_k)=Q_k^{(m)}(R_k) \tag{16}$$

$$U_k^{(m)}(R_k)=\frac{R_k^2}{2^2}+\frac{R_k^3}{3^2}+\ldots+\frac{R_k^{m+2}}{(m+2)^2} \tag{17}$$

Using equations (14) and (16), integral (11) change to the following form:

$$I_\Omega(X')=\sum_{k=1}^{N}\alpha_k\int_\Omega G(X,X')\nabla^2 U_k^{(m)}(R_k)\,d\Omega \tag{18}$$

The domain integral in the equation (18) can be changed to boundary integral by using again the second form of Green's theorem:

$$\int_\Omega G(X,X')\nabla^2 U_k^{(m)}(R_k)\,d\Omega=-C(X')U_k^{(m)}(R'_k)+\oint_\Gamma G(X,X')\frac{\partial U_k^{(m)}(R_k)}{\partial n}-U_k^{(m)}(R_k)\frac{\partial G(X,X')}{\partial n}d\Gamma \tag{19}$$

where $R'_k=|X'-X_k|$. By putting equation (19) in equation (18) it can be derived that:

$$I_\Omega(X')=\sum_{k=1}^{N}\alpha_k F_k(X') \tag{20}$$

where:

$$F_k\left(X'\right) = -C\left(X'\right)U_k^{(m)}\left(R'_k\right) + \oint_\Gamma G\left(X,X'\right)\frac{\partial U_k^{(m)}\left(R_k\right)}{\partial n} - U_k^{(m)}\left(R_k\right)\frac{\partial G\left(X,X'\right)}{\partial n}d\Gamma \quad (21)$$

It can be seen that $F_k\left(X'\right)$ for each arbitrary point of X' in the domain of Ω can be calculated, and the regional integral (11) is converted into a series of boundary integrals.

4 Boundary integrals

At first, the Γ boundary is gridding in order to calculate the boundary integrals in equations (12) and (13). Boundary element with index i is consider as connecting line between any two points of the set of sampling points that are located on the Γ boundary. As a result, the boundary integrals (12) and (13) are converted into the summation of integrals over each boundary element:

$$I_{1\Gamma}\left(X'\right) = \sum_{i=1}^{N_B}\int_{\Gamma_i} G\left(X,X'\right)\frac{\partial U\left(X\right)}{\partial n}d\Gamma \quad (22)$$

$$I_{2\Gamma}\left(X'\right) = \sum_{i=1}^{N_B}\int_{\Gamma_i} U\left(X\right)\frac{\partial G\left(X,X'\right)}{\partial n}d\Gamma \quad (23)$$

where N_B expresses the number of boundary elements. Function of $U\left(X\right)$ on the Γ_i boundary element can be approximated as the following:

$$U\left(X\right)|_{\Gamma_i} \approx \frac{1-\alpha}{2}U_{i-1} + \frac{1+\alpha}{2}U_i \quad (24)$$

Parameter of α varies in the range of $[-1,1]$ and parametric equation of Γ_i boundary element can be expressed by α as the following:

$$x\left(\alpha\right)|_{\Gamma_i} \approx \frac{1-\alpha}{2}x_{i-1} + \frac{1+\alpha}{2}x_i \quad (25)$$

$$y\left(\alpha\right)|_{\Gamma_i} \approx \frac{1-\alpha}{2}y_{i-1} + \frac{1+\alpha}{2}y_i \quad (26)$$

According to the relations (25), and (26), it can be derived that:

$$d\Gamma = \sqrt{\left(dx\right)^2 + \left(dy\right)^2} = \frac{L_i}{2}d\alpha \quad (27)$$

where L_i is the length of the Γ_i boundary element. By using the equations (24), (25), (26) and (27), $I_{2\Gamma}\left(X'\right)$ can be calculated. To calculate each of the integrals of equation (22), some points (except starting and ending points) is selected as nodes on the element of Γ_i. With regard to number of selected nodes on the element, function of $\partial U\left(X\right)/\partial n$ can be estimated. In this study, linear elements approximation is used. In this approximation, 2 nodes are considered on each element. The coordinates of the nodes are shown with $X_i^{(1)}$ and $X_i^{(2)}$. The values of $\partial U\left(X_i^{(1)}\right)/\partial n$ and $\partial U\left(X_i^{(2)}\right)/\partial n$ represented with $q_i^{(1)}$ and $q_i^{(2)}$, respectively. In the linear elements approximation, $\partial U\left(X\right)/\partial n$ is expressed as follows [8]:

$$\left.\frac{\partial U\left(X\right)}{\partial n}\right|_{\Gamma_i} = W_1\left(\alpha\right)q_i^{(1)} + W_2\left(\alpha\right)q_i^{(2)} \quad (28)$$

where weighting functions of $W_1\left(\alpha\right)$ and $W_2\left(\alpha\right)$ are linear functions that their functional shape are specified with respect to the location of the $X_i^{(1)}$ and $X_i^{(2)}$ nodes. For example, by choosing nodes at locations of 1/4 and 3/4 lengths of each element, these functions are expressed as follows:

$$W_1\left(\alpha\right) = \frac{1-2\alpha}{2} \quad (29)$$

$$W_2\left(\alpha\right) = \frac{1+2\alpha}{2} \quad (30)$$

By putting the equations (25), (26), (27) and (28) in equation (22) it derives that:

$$I_{1\Gamma}\left(X'\right) = \sum_{i=1}^{N_B}\int_{-1}^{1} G\left(X\left(\alpha\right),X'\right)\left\{W_1\left(\alpha\right)q_i^{(1)} + W_2\left(\alpha\right)q_i^{(2)}\right\}\frac{L_i}{2}d\alpha \quad (31)$$

This equation can be arranged as follows:

$$I_{1\Gamma}\left(X'\right) = \sum_{i=1}^{N_B} A_i^{(1)}\left(X'\right)q_i^{(1)} + A_i^{(2)}\left(X'\right)q_i^{(2)} \quad (32)$$

where:

$$A_i^{(1,2)}\left(X'\right) = \int_{-1}^{1} G\left(X\left(\alpha\right),X'\right)W_{1,2}\left(\alpha\right)\frac{L_i}{2}d\alpha \quad (33)$$

5 Solving the integral equation

By putting the equations (20), (23) and (32) in equation (10) it derives that:

$$C\left(X'\right)U\left(X'\right) = -I_{2\Gamma}\left(X'\right) - \sum_{k=1}^{N}\alpha_k F_k\left(X'\right) + \sum_{i=1}^{N_B} A_i^{(1)}\left(X'\right)q_i^{(1)} + A_i^{(2)}\left(X'\right)q_i^{(2)} \quad (34)$$

where the coefficients of α_k, $q_i^{(1)}$ and $q_i^{(2)}$ are unknown. By selecting of observation point X' on each sampling

points of $X_{k'}$ and node points of $X_{i'}^{(1)}$ and $X_{i'}^{(2)}$, equation (34) is changed to an algebraic system of equations. Consequently, an algebraic system of equations with $N+2N_B$ is obtained:

$$-\sum_{k=1}^{N}\alpha_k F_k(X_{k'}) + \sum_{i=1}^{N_B} A_i^{(1)}(X_{k'})\,q_i^{(1)} + A_i^{(2)}(X_{k'})\,q_i^{(2)} = C(X_{k'})\,U(X_{k'}) + I_{2\Gamma}(X_{k'}) \quad (35)$$

$$-\sum_{k=1}^{N}\alpha_k F_k\left(X_{i'}^{(1)}\right) + \sum_{i=1}^{N_B} A_i^{(1)}\left(X_{i'}^{(1)}\right) q_i^{(1)} + A_i^{(2)}\left(X_{i'}^{(1)}\right) q_i^{(2)} = C\left(X_{i'}^{(1)}\right) U\left(X_{i'}^{(1)}\right) + I_{2\Gamma}\left(X_{i'}^{(1)}\right) \quad (36)$$

$$-\sum_{k=1}^{N}\alpha_k F_k\left(X_{i'}^{(2)}\right) + \sum_{i=1}^{N_B} A_i^{(1)}\left(X_{i'}^{(2)}\right) q_i^{(1)} + A_i^{(2)}\left(X_{i'}^{(2)}\right) q_i^{(2)} = C\left(X_{i'}^{(2)}\right) U\left(X_{i'}^{(2)}\right) + I_{2\Gamma}\left(X_{i'}^{(2)}\right) \quad (37)$$

where $k' \in \{1,\ldots,N\}$ and $i' \in \{1,\ldots,N_B\}$. By solving this system, the coefficients of α_k, $q_i^{(1)}$ and $q_i^{(2)}$ can be obtained. By using these coefficients in equation (34), value of $U(X')$ can be calculated at any arbitrary point within a specific area.

6 Numerical result analysis

In order to evaluate the precision and accuracy of the presented method in this paper, numerical sampling from some specific functions has done and by using the sampling data, interpolation has done. Then, in more than 1000 points, the interpolation values compared with the primary function values. For this comparison, the following parameters were calculated:

$$AVG = \frac{1}{N_T}\left(\sum_{j=1}^{N_T}\left|\bar{U}(X_j)\right|\right)$$

$$ERR = \frac{1}{N_T}\left(\sum_{j=1}^{N_T}\left|\bar{U}(X_j) - U(X_j)\right|\right)$$

$$RMSE = \sqrt{\frac{1}{N_T}\left(\sum_{j=1}^{N_T}\left(\bar{U}(X_j) - U(X_j)\right)^2\right)}$$

Table 1: Interpolation by primary function of $\sin(x)\sin(y)$ for different values of m.

M	AVG	ERR	RMSE	R-RMSE
1	0.202	$1.545e-3$	$2.610e-3$	1.290
2	0.202	$1.407e-3$	$2.916e-3$	1.441
3	0.202	$1.200e-3$	$2.330e-3$	1.152
4	0.202	$1.381e-3$	$2.702e-3$	1.336
5	0.202	$1.481e-3$	$2.667e-3$	1.318
6	0.202	$1.506e-3$	$2.708e-3$	1.338
7	0.202	$1.434e-3$	$2.989e-3$	1.478
8	0.202	$1.975e-3$	$4.401e-3$	2.175
9	0.202	$2.631e-3$	$6.228e-3$	3.078

Table 2: Interpolation by primary function of x^2+y^2 for different values of m.

M	AVG	ERR	RMSE	R-RMSE
1	0.633	0.032	0.042	6.634
2	0.633	0.034	0.044	6.990
3	0.633	0.048	0.063	9.886
4	0.633	0.061	0.082	12.885
5	0.633	0.028	0.04	6.339
6	0.633	0.019	0.035	5.594
7	0.633	0.023	0.043	6.724
8	0.633	0.017	0.037	5.781
9	0.633	0.207	0.251	39.669

$$R-RMSE = (RMSE/AVG)\times 100$$

where X_j is location of estimated points and N_T is the number of theses points. These quantities express the mean absolute of primary function at the estimated points, mean absolute error of interpolation function to the primary function, root mean square error, and its percentage, respectively. At the first problem, from the function of $\bar{U}(X) = \sin(x)\sin(y)$ sampling has done in $N = 7\times 7$ points with square pattern in the interval $x \in [-1,1]$ and $y \in [-1,1]$ (Figure 2-b). 24 points ($N_B = 24$) from the total points are located on the boundary and 25 points ($N - N_B = 25$) of them are located inside the boundaries. Results of interpolation for different values of m (polynomial order of the expansion $Q(X)$ in equation 14) are given at Table 1. According to Table 1, it can be observed that the values of mentioned quantities experience a lot of variation relative to the parameter m. In addition, the differences of the interpolation function is very small compared to the primary function and the best interpolation is performed at $m = 3$. At all estimation points, interpolation is done by inverse optimal distance method according to the following equation:

$$U(X) = \left(\sum_{k=1}^{N} U_k d_k^{-\beta}\right) / \left(\sum_{k=1}^{N} d_k^{-\beta}\right)$$

The following results obtained from comparison of the interpolation values with primary function values at

Table 3: Interpolation by primary function of x^2-y^2 for different values of m.

M	AVG	ERR	RMSE	R-RMSE
1	0.316	7.739e-3	9.758e-3	3.087
2	0.316	0.013	0.017	5.254
3	0.316	0.035	0.047	14.892
4	0.316	4.954e-3	9.48e-3	3
5	0.316	4.043e-3	6.563e-3	2.077
6	0.316	—	—	—
7	0.316	3.929e-3	6.481e-3	2.051
8	0.316	0.013	0.016	5.197
9	0.316	0.075	0.097	30.773

Table 4: Interpolation by primary function of $\sin(2x)\cos(3y)$ for different values of m.

M	AVG	ERR	RMSE	R-RMSE
1	0.429	0.049	0.077	17.941
2	0.429	0.045	0.068	15.908
3	0.429	0.031	0.048	11.204
4	0.429	0.033	0.049	11.521
5	0.429	0.023	0.036	8.349
6	0.429	0.029	0.045	10.518
7	0.429	0.019	0.033	7.588
8	0.429	0.074	0.151	35.247
9	0.429	0.019	0.027	6.2

Table 5: Interpolation by different primary functions, with optimal values of m for different sampling point arrangements. A: $\sin(2x)\cos(3y)$, B: $\exp\left(-4(x^2+y^2)\right)$, C: $\sin^2(2xy)\exp\left(-4(x^2+y^2)\right)$,

Function	N	M	AVG	ERR	RMSE	R-RMSE
A	49	9	0.429	0.019	0.027	6.2
A	91	8	0.385	6.052e-3	0.012	3.07
A	106	6	0.395	8.318e-3	0.016	3.989
B	41	1	0.303	4.052e-3	5.429e-3	1.79
B	60	1	0.269	8.756e-3	0.013	4.734
B	106	1	0.241	6.387e-4	1.089e-3	0.452
C	41	1	0.407	0.027	0.039	9.466
C	49	5	0.468	0.022	0.032	6.88
C	91	5	0.388	5.387e-3	8.704e-3	2.241

$\beta = 3$: $ERR = 0.024$, $RMSE = 0.03$, $R-RMSE = 14.855$. By comparing these results with the results of Table 1 it can be seen that in this problem, interpolation by this method is more accurate than inverse distance method. In the following, sampling is performed on three functions of $\bar{U}_1(X) = x^2+y^2$, $\bar{U}_2(X) = x^2-y^2$ and $\bar{U}_3(X) = \sin(2x)\cos(3y)$ as primary functions at specified locations shown in Fig. (2-a). Then, interpolation is carried out based on this method for different values of m and the primary function values are compared with the calculated values (Tables 2, 3 and 4). The best values of interpolation for functions $\bar{U}_1$, $\bar{U}_2$ and $\bar{U}_3$ are carried at $m=6$, $m=7$ and $m=9$, respectively. In many two-dimensional interpolation problems, location of sampling points is sparse. One of the advantages of this method is that the regular or scattered location of the sampling points is not important in the interpolation process. Furthermore, in this method after solving equations system (35), (36) and (37) it is reachable to calculate value of interpolation function at any arbitrary points in the area of interest according to equation (34). Continuity of the interpolation function is another advantage of this method. In addition, it is obvious according to equation (34), interpolation function and its partial derivatives are continuous in whole of the domain. To further investigate the results of this method, interpolation has done with the primary functions and different points sampling patterns. Two regular arrangements with 49 and 91 points and three non-regular patterns with 41, 60 and 106 points are considered (Fig. 2). The primary functions and applied arrangement type in the sampling are described in Table (5). In all cases, the interpolation is carried out for different values of m from 1 to 9 and the optimal value of this parameter for each interpolation is reported in Table (5). It observed that with variation of primary function and pattern of sampling points, optimal value of the parameter has changed. By comparing of second and third lines of this table, it can be seen that however in the 106 points arrangement, there is large number of points but at the 91 points arrangement there is better result due to regularity of location of points. In addition, with regard to Fig. 2 and comparison of fourth and fifth lines, it is clear that result of interpolation from 41 points arrangement is better than 60 points arrangement due to asymmetric distribution of points in 60 points arrangement. Regular arrangement of sampling points at two last lines is selected and it shows there is a better interpolation due to increase number of points. Besides, Table (6) shows the results of three other interpolation methods, i.e., Inverse Distance Method, Nearest Neighbor Method, and Moving Average Method, for some of the mentioned primary functions in Table (5). Comparison of these Tables (Table 5 and Table 6)

Table 6: Interpolation by different primary functions for different sampling point arrangements using three estimators. IDM: Inverse Distance Method $\beta = 3$, NNM: Nearest Neighbor Method, MAM: Moving Average Method,

Function	N	AVG	ERR	RMSE	R-RMSE
IDM					
A	49	0.276	0.170	0.220	79.7
B	60	0.263	0.096	0.137	52.1
C	49	0.009	0.003	0.004	44.4
NNM					
A	49	0.449	0.142	0.178	39.6
B	60	0.234	0.046	0.066	28.2
C	49	0.009	0.004	0.005	55.6
MAM					
A	49	0.351	0.492	0.297	84.6
B	60	0.287	0.252	0.286	99.6
C	49	0.008	0.007	0.007	87.5

demonstrates that the current interpolation method, i.e, Dual Reciprocity Boundary Element Method, has better results based on R-RMSE parameter.

7 Conclusions

A numerical method based on Dual Reciprocity Boundary Element Method (DRBEM) has presented to interpolate scattered data with arbitrary pattern. Numerical sampling has conducted on some specific functions as primary functions and interpolation values of numerical sampling have compared to primary function values to evaluate accuracy and precision of the method. In some cases, the results of other interpolation methods are compared with this method. However, one of the advantages of this method is that there is no difference in calculation method of data with regular or non-regular arrangement. It is important to mention that as much as sampling done better, the accuracy of interpolation will increase. Another advantage of this method is that interpolation is done without need to any specific boundary condition. Moreover, due to the fact that this method is based on the boundary integral equations, everyone can attain his/her purpose in a very short time using personal computers.

References

[1] J. Li, A. D. Heap, Geoscience Australia, **23**, 137 (2008).
[2] S. R. Karur, P. A. Ramachandran, Mathematical and Computer Modelling, **20**, 59 (1994).
[3] I. P. Agnantiaris, D. Polyzos, D. E. Beskos, Computational Mechanics, **17**, 270 (1996).
[4] M. A. Golberg, C. S. Chen, H. Bowman, H. Power, Computational Mechanics, **22**, 61 (1998).
[5] G. Fairweather, A. Karageorghis, Advances in Computational Mathematics, **9**, 69 (1998).
[6] M. A. Golberg, C. S. Chen, H. Bowman, Engineering Analysis with Boundary Elements, **23**, 285 (1999).
[7] C. Gaspar, Engineering Analysis with Boundary Elements, **24**, 559 (2000).
[8] F. Paris, J. Canas, Oxford University Press, (1997).
[9] M. J. D. Powell, A Review in IMA Conference on Algorithms for the Approximation of Functions and Data, RMCS, Shrivenham, 143 (1985)
[10] C. A. Micchelli, Constructive Approximation, **2**, 11 (1986).